Characterization of single Au and SiO_2 nano- and microparticles by ICP-OES using monodisperse droplets of standard solutions for calibration

Carmen C. Garcia,†* Ayrat Murtazin, Sebastian Groh, Vlasta Horvatic‡ and Kay Niemax

Received 7th October 2009, Accepted 23rd December 2009
First published as an Advance Article on the web 21st January 2010
DOI: 10.1039/b921041e

The masses of single SiO_2 and Au nano- and microspheres were measured by introducing monodisperse droplets of diluted Au and SiO_2 particle suspensions into an ICP-OES system and calibrating the element line intensities by respective intensities obtained with monodisperse droplets of Si and Au standard solutions with known concentrations and diameters. Commercially available SiO_2 (diameters between 470 nm and 2.06 μm) as well as 250 nm Au particles, both with small size dispersions, were used in the investigations. Evaluation of the ICP-OES signals revealed good agreement between the atomic line intensities recorded with particles and droplets from standard solutions having the same analyte mass as the particles. Detection limits of spherical solid particles by ICP-OES were found to be ~200 nm and ~470 nm for Au and SiO_2 particles, respectively. The corresponding analyte masses at the detection limits were ~80 fg (Au) and ~50 fg (Si). The general applicability of the suspension technique for measurements of nanoparticles having different sizes and masses is demonstrated analyzing a suspension containing spherical SiO_2 particles of three different sizes.

Introduction

Nanoparticles (NPs) have significant potential to bring benefits to many areas of research and application. Important technical applications are, *e.g.*, their use as catalysts,[1] improving the efficiency of fuel cells and batteries, as lubricants, where nanospheres of inorganic materials act as nanosized "ball bearing"[2,3] or as surface coating.[4] However, even more important are their biomedical applications, for example, in medical diagnostics and treatment.[5]

On the other hand, the use of NPs does not only bring benefits. Ultrafine particles, present as airborne aerosols or as particles in suspensions, can also have a strong impact on environment and health.[5,6] For example, they can easily penetrate through cell membranes into biological cells[7] where they induce biochemical reactions due to their chemical reactivity and their large surface to mass ratio.

Most analytical methods currently used for NP characterization are "off-line" techniques. They are time-consuming since there are several preparation steps before measurement. Among the off-line methods one can find electron beam or scanning probe techniques. Here, transmission electron microscopy (TEM) and scanning electron microscopy (SEM) are the most popular electron beam techniques. On the other hand, scanning probe microscopy (SPM), scanning tunneling microscopy (STM), and atomic force microscopy (AFM) are the most popular scanning probe techniques.[8] Furthermore, there are commercial instruments available which provide simultaneous information on particle size and composition using integrated filtration, imaging and spectroscopic techniques, such as Raman spectroscopy or laser induced breakdown spectroscopy (LIBS). However, all these techniques cannot give analytical information on particles much smaller than 1 μm.

It has to be noted that the most popular methods for on-line characterization of NPs provide only size and shape information. Here, we can find particle impaction instruments, differential mobility analysers (DMA) and optical particle sizing devices. However, other techniques which provide limited information about particle composition have to be mentioned as well. These are, for example, electrical low-pressure impaction, static diffractometry or diffusion batteries.[8] The review paper by Burleson *et al.*[9] gives an excellent overview on today's characterization techniques for environmental particles providing information from the nanometre to the micrometre scale length. It is particularly stressed that multiple techniques are usually employed for particle characterization.

An interesting instrument for fast particle analysis is the Aerosol Time of Flight Mass Spectrometer (A-TOFMS) (Company: TSI Incorporated). The A-TOFMS uses an aerodynamic sizing technique to measure individual particles which are subsequently desorbed and ionized by laser vaporization. Analyses are performed by time-of-flight mass spectrometry. This instrument detects and analyzes particles in the size range from 0.3 to 3 μm.[10] However, quantification is certainly a problem as in all laser ablation techniques.

Laser induced breakdown spectrometry (LIBS) for particle characterization was first demonstrated by Radziemski and

Plasma-Analyte Interaction Working Group (PAIWG)§ of ISAS – Institute for Analytical Sciences at the Technical University of Dortmund, Bunsen-Kirchhoff-Strasse 11, 44139 Dortmund, Germany. E-mail: Carmen.GARCIA-PEREZ@ec.europa.eu; niemax@isas.de

† Now with European Commission, Joint Research Centre, Institute for Transuranium Elements, Karlsruhe, Germany.

‡ Permanent address: Institute of Physics, Bijenicka 46, 10000 Zagreb, Croatia.

§ PAIWG is a collaborative effort of the University of Florida (Gainesville, USA), the Federal Institute for Materials Research and Testing (BAM, Berlin, Germany) and ISAS in Dortmund, jointly funded by NSF and DFG.

co-workers in the early 1980s.[11] More recently, in particular Hahn and his group at the University of Florida studied the laser induced plasma vaporization of airborne particles using LIBS.[12,13] Whenever single particles crossing the volume where the pulsed laser breakdown occurs are interacting with the laser, emission spectra of the particle constituents can be recorded.

The basic idea applying ICP-OES for characterization of airborne nano- and microparticles was first presented by Kawaguchi *et al.*[14] in 1986. They investigated the possibility to calibrate intensity spikes from copper particles with aerosols generated from monodisperse droplets of copper solution (diameter: slightly below 40 μm). Later, Knight *et al.*[15] made the attempt to correlate size and composition of microparticles with optical emission signals of the elements. Unfortunately, this work was not fully successful because the injected silica (diameter: 3 and 7.6 μm), zircon and albite particles were obviously not completely vaporized. Furthermore, the authors were not sure about the particle size distributions. Nevertheless, it was shown that this method is able to discriminate particles of different composition in complex mixtures.

Introduction of particles from desolvated monodisperse droplets of standard solution into an ICP has also been investigated by Olesik[16] applying side-on optical emission spectrometry (OES). These experiments were performed for studying the atomization processes in the ICP and better understanding of matrix effects.

At ISAS we are investigating the possibility to characterize the mass and element composition of NPs by ICP spectrometry using monodisperse droplets of standard solutions for calibration.[17] The project was established after first promising measurements of individual particles by ICP-OES in our laboratory.[18] In that particular experiment, particles produced by laser ablation of brass were detected by simultaneous measurement of strong Cu and Zn lines. However, the element masses and their ratios in the individual particles could not be determined because calibration standards for NPs are generally not available.

One experimental approach at ISAS for characterization of airborne particles is similar to the procedure published by Kawaguchi *et al.*[14] and Olesik and his group,[16] where monodisperse microdroplets of standard solutions are desolvated before the residua are introduced as particles into the ICP. The analyte signals of the dry residua are then compared with the signals obtained with the airborne particles of interest. In the other experimental approach, which is the subject of the present paper, the NPs of interest are in a liquid, *e.g.*, in deionized water. This suspension is diluted and put into an ultrasonic device to avoid agglomeration of particles. The particle suspension is then introduced to the ICP in the form of monodisperse microdroplets. The particle concentration in the suspension has to be so low that most droplets do not include any particle and the probability of having two or more particles in one droplet can be neglected. Subsequently, the element signals from droplets with particles are calibrated by respective signals measured with monodisperse droplets of known size and standard solution.

Well characterized particles are required in order to study the possibilities and limitations of the technique. Therefore, SiO_2 and Au micro- and nanospheres were used as test particles in the present study. Both types of NPs are commercially available in suspension having small size dispersions.

Experiment

The experimental arrangement is shown in Fig. 1. It is the same as recently used for the investigation of atomization processes of monodisperse droplets from standard solutions.[17] Therefore, we refer to the detailed experimental information given in that reference and will only give the most important features of the arrangement here.

Monodisperse microdroplets are generated from standard solutions or from particle suspensions applying a commercial piezo-electric droplet dispenser (Type MD-E-201 H with dispenser head MD-K-150, microdrop Technologies, Norderstedt, Germany). The dispenser head is equipped with gas nozzles (dispenser gas flow) around the orifice for droplet production. Throughout the experimental investigations the smallest commercially available orifice (diameter: 30 μm) was used generating monodisperse droplets with diameters of about 50 μm for the chosen piezo-electric pulse parameters (voltage and length). The variation of the diameter for successive droplets is very small (<1% as claimed by the manufacturer). However, a visual control of droplet production, diameter and velocity is required. For this purpose, the droplets were stroboscopically illuminated and measured with a commercial microscope with CCD camera delivered together with the droplet dispenser. The accuracy of the droplet diameter measurements was about ±3 μm, limited by the pixel size of the CCD. A droplet generation rate of 10 Hz or 20 Hz was used throughout the experiment.

Once the stability of droplet generation was established, droplets made from element standard solutions or particle suspensions were transported by a dispenser gas flow of 0.21 L min^{-1} Ar directly through the injector tube (diameter at the end: 1 mm) of the vertically mounted ICP torch into the plasma. A silicone o-ring between the dispenser head and the injector tube was applied to tighten the units. Note that the injector flow rate is lower than usually applied in ICP spectrometry. The low gas flow rate, however, was necessary because of two reasons. First, the droplet transport became unstable for flow rates larger than ~0.3 L min^{-1} and second, the residence time of the droplets with analyte solution or particles in the ICP had to be long enough that atomization and plasma equilibration can be accomplished.[17]

The ICP with power supply unit was taken from a prototype ICP-instrument (ELEMENT 1, Finnigan MAT, Bremen,

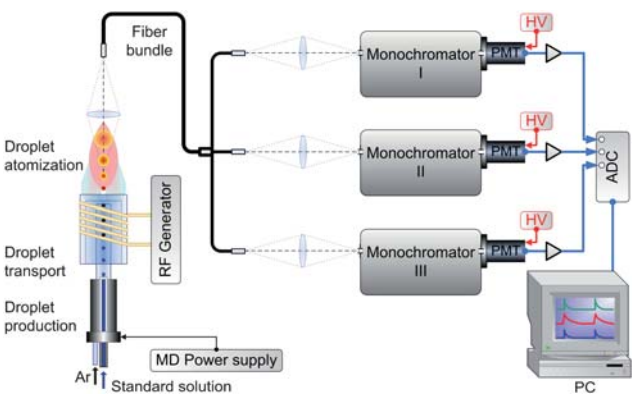

Fig. 1 Experimental arrangement used for particle characterization.

Table 1 Operating conditions of the ICP-OES system

Parameter	Value/Model
ICP (ELEMENT 1, Finnigan MAT)	
RF forward power	1000 W
Plasma gas (Ar) flow rate	16 L min^{-1}
Auxiliary gas (Ar) flow rate	1 L min^{-1}
Dispenser gas (Ar) flow rate	0.21 L min^{-1}
OES system	
Monochromator 1	Jobin-Yvon SPEX 1000M
Grating	2400 groves/mm
Slit	100 μm
Photomultiplier 1	EMI 9789 QA
Voltage	1000V
Monochromator 2	McPherson 2051
Grating	2400 groves/mm
Slit	100 μm
Photomultiplier 2	EMI 9784 QA
Voltage	1000V
Monochromator 3	McPherson EU 700
Grating	1200 groves/mm
Slit	50 μm
Photomultiplier 3	EMI 9789 QA
Voltage	900V

Germany). Operation conditions for the ICP-OES measurements are summarized in Table I. The generated spectral emission was collected end-on and focused onto a quartz fiber bundle which splits the light into three equal parts for three different monochromators equipped with fast photomultiplier tubes. Stanford Research SR570 amplifiers were coupled to each photomultiplier. The amplified signals were digitized (National Instruments DAQPad-6015) and processed.

The SiO_2 particles were analyzed by tuning the Spex monochromator (see Table I) to the Si(I) 288.16 nm and the McPherson 2051 to the Ca(II) 393.36 nm emission lines, respectively. A time constant of 5.3 μs in both amplifiers was found to be the optimum for the silica particles measurements fixing the data acquisition rate to 60 kHz. For the analysis of the 250 nm Au particles, the Au(I) emission line at 267.59 nm was measured using the 1 m-SPEX monochromator, while the Ca(II) emission line at 393.36 nm was again monitored with the McPherson 2051. Here, the time constant and the sample rate were 0.53 ms and 10 kHz, respectively. The Ca(II) line was used as internal marker for spectroscopic registration of the droplet injection frequency and for coincidence control of droplets with and without particles. Therefore, small amounts of calcium were added to the solutions or suspensions in both measurements.

The third monochromator (EU 700) was used in some of the measurements, in particular, when a second Si or Au line had to be monitored simultaneously.

Samples

Diluted suspensions of monodisperse Au and SiO_2 particles were prepared from commercially available suspensions. Suspensions of monodisperse 0.53, 0.873, 1.16, 1.55, and 2.06 μm SiO_2 particles having coefficients of variation (CV) of ~4.7%, ~4.7%, 4.2%, 2.3%, and 2.2%, respectively were purchased from microParticles GmbH (Berlin, Germany), while the 250 nm Au particles suspension was delivered by Microspheres-Nanospheres (Corpuscular, Cold Spring, NY, USA). The Au particle suspension, stabilized by $HAuCl_4$, had a concentration of 3.6×10^8 particles per mL and a CV of the particle diameter of 8%. The diameters and the monodispersity of the commercial particles were measured using a Quanta 200F scanning electron microscope (FEI). The nominal diameters of all particles could be verified within the experimental uncertainty. Only the nominal diameter of the 530 nm and 873 nm SiO_2 particles could not be confirmed by SEM measurements which gave slightly smaller average diameters (470 nm and 830 nm, respectively). Therefore, the values 470 nm and 830 nm instead of 530 nm and 873 nm are used throughout the paper.

The undiluted suspensions were put in an ultrasonic bath for about 30–60 min to minimize agglomeration and sedimentation of particles. In the next step, the suspensions were diluted with deionized water in order to have on average less than 1 particle in each 50 μm droplet produced by the droplet generator. After dilution and before each analysis the samples were again treated in the ultrasonic bath for ~20 min. Once the suspensions were properly diluted and the generated droplets visually controlled, the droplet dispenser was directly attached to the injector of the ICP torch and the droplets were transported by the dispenser gas flow into the plasma.

For quantification of the particle signal, aqueous gold and silicon solutions were prepared from standards of 1000 μg mL^{-1} Au in 20% HCl (Johnson Matthey GmbH, Alfa Products) and 1000 μg mL^{-1} Si as $(NH_4)_2SiF_6$ in water (Merck KGaA). The diluted SiO_2 suspensions were doped with 100 ng mL^{-1} Ca prepared from a calcium standard solution of 1000 μg mL^{-1} in 5% HNO_3 (Johnson Matthey GmbH, Alfa Products). Ca doping was not necessary in some of the Au particle measurements since the calcium concentration in the original suspension was already sufficiently high for monitoring.

Results and discussion

Characterization of SiO_2 particles by ICP-OES

Fig. 2 shows the line intensities of Si (part b) and the Ca (part a) at 288.16 nm and 393.36 nm, respectively, measured simultaneously

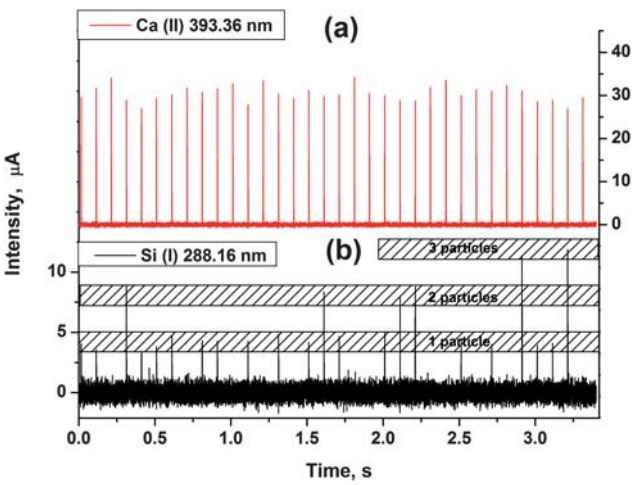

Fig. 2 ICP-OES signals of silicon and calcium measured with monodisperse 47 μm droplets of a 100 μg mL^{-1} Ca solution (a) including one, two or three 830 nm SiO_2 particles (b). The intensity intervals for one, two and three particles are hatched in (b).

by introducing monodisperse 47 μm droplets of a Ca spiked, diluted suspension of monodisperse 830 nm SiO_2 particles. The reproducibility of droplet injection at 10 Hz production rate can be read from the Ca signal in Fig. 2a. While standard deviation of the temporal fluctuation of the periodicity was on the order of 6%, the typical fluctuation of the peak intensity was larger (~10%). The relatively strong peak intensity fluctuation is surprising since Olesik and Hobbs[19] reported on standard deviations of 1–6% in side-on line intensity measurements applying monodisperse droplet introduction. Only when the volume where atomization occurred was imaged, the standard deviation was larger. We believe that the present, relatively large standard deviation of the Ca peak intensities is primarily due to fluctuations reported by Olesik and Hobbs. However, also slightly different trajectories of consecutive droplets in the ICP might contribute to the standard deviation. On the other hand, the Si signal is also affected by background noise which is a minor contribution to the Ca intensities because of the large signal to noise ratio. Note that the same imaging conditions were used as in the recent end-on studies on droplet atomization in the ICP.[17] They were set by optimizing the peak intensity, *i.e.*, by imaging the analyte cloud at a very early stage where line emission from as many excited atoms as possible was collected. Slightly different trajectories have a much larger effect on the measured intensity than when a larger analyte cloud at later time downstream the ICP is imaged. This might explain why the standard deviation of the integral intensities of the same, end-on measured peaks had significantly lower standard deviations (~5%) than the peak measurements. However, it has to be noted that the standard deviation of peak intensity measurements can also be significantly lower than ~10%. Recently, a standard deviation of 3.1% was found in measurements with relatively high Ca concentrations by carefully optimizing the gas flow ratios of injector, plasma and auxiliary gas.[20] The standard deviation of area measurements was 2.5% in that experiment. Unfortunately, these optimum conditions are not very stable and are hard to reproduce from measurement to measurement, probably due to small differences of the gas flows. A more detailed discussion on other possible reasons for the signal fluctuations is given below.

Si emission signals coinciding with the droplet marker, the Ca peaks, were only measured from time to time depending on the particle concentration in the suspension. Fig. 2b shows the measurement of 34 consecutive droplets, 22 droplets include SiO_2 particles. Taking into account already this limited number of droplets, it can be seen that 16 droplets include one SiO_2 particle, in four droplets are two particles each, and in two droplets three particles. The probability of finding none ($k = 0$), one ($k = 1$) or more particles ($k = 2,3,\ldots$) in the droplets is given by Poisson statistics $P_\lambda(X = k) = \frac{\lambda^k}{k!}e^{-\lambda}$, where λ is the ratio of the number of particles in a suspension to the number of droplets representing the total volume of the suspension. The precondition for application of Poisson statistics is that the particles are statistically distributed in the suspension, *i.e.*, that there is no agglomeration. We will see later that stronger dilution will reduce the probability of finding more than one particle in a droplet which is a requirement to discriminate particles with different mass in suspensions by the droplet injection method.

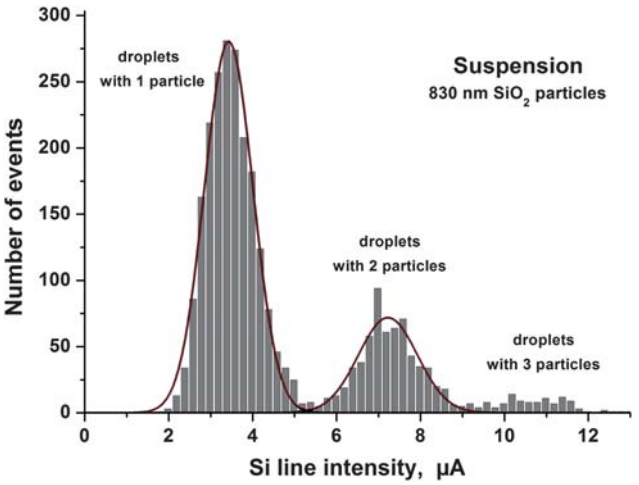

Fig. 3 Histogram of the peak intensities of the Si 288.16 nm line measured with a diluted suspension of 830 nm SiO_2 particles.

The evaluation of a much larger number of Si peaks measured with the same suspension of 830 nm SiO_2 particles as in Fig. 2 is shown in Fig. 3. The number of peaks in small, chosen intensity intervals is plotted in dependence on peak intensity. The intensity distributions belonging to one and two particles were fitted by Gauss functions although there is a small asymmetry in the signal distribution for one particle. Evaluating the centers of gravity the average intensities (3.43 and 7.33 μA) scale as 1 : 2.1. The standard deviations for the measurement of one and two particles were ±0.58 and ±0.71, respectively. Note that the Si mass of a single particle is 257 fg taking into account the SiO_2 density of 1.85 g cm^{-3}.

Peak intensity distributions measured with the same particle suspension but with addition of a Si standard solution are displayed in Fig. 4. Here, the first distribution is produced by droplets of Si solution (diameter: 47 μm; Si concentration: 4.55 μg mL^{-1}) without particles, while the second and third mark solution droplets with one and two particles, respectively. The Si

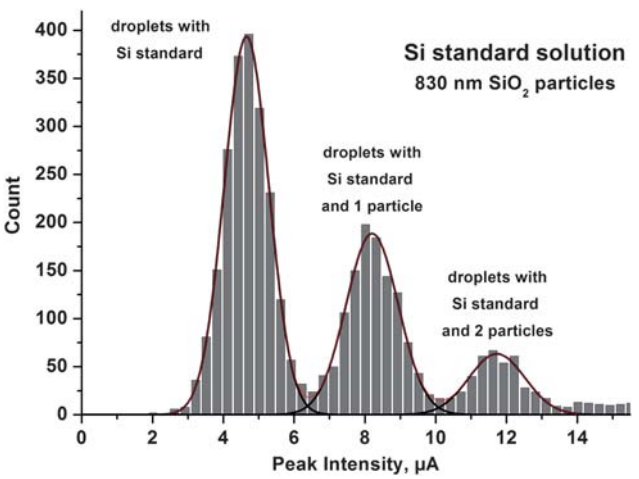

Fig. 4 Histogram of the peak intensities of the Si 288.16 nm line measured with a Si standard solution (Si concentration: 4.55 μg mL^{-1}) including 830 nm SiO_2 particles.

mass solved in single droplets is 247 fg which is close to the Si mass in individual 830 nm particles (257 fg). The averaged intensities in Fig. 4 (4.65 ± 0.63, 8.21 ± 0.74, and 11.73 ± 0.79) are reflecting the expected Si mass ratios (1 : 1.91 : 2.84) within the limits of experimental uncertainty which indicates that the Si mass in SiO_2 particles can be measured by calibration with monodisperse droplets of known size and Si concentration. However, it should be noted that there is a slight intrinsic systematic error in the comparison of Si masses in droplets of solution only and in droplets of solution including particles. While the maximum of the calibration peak should exactly correspond to the Si mass in a 47 μm droplet because of the high monodispersity of the droplets, the peaks of the droplets with one and two particles cannot be directly compared because there is a significant variation of the particle size. Regarding the r^3-dependence of the mass of spherical particles and assuming, *e.g.*, a Gaussian particle size distribution with a CV of a few percent, the averaged particle mass presented by the measured peak in the histogram is slightly higher than the mass which is calculated by taking only the mean diameter into account.

We believe that the standard deviation of the Si mass determination for 830 nm particles is mainly due to the relatively large background noise, since the scatter of the peak intensity measured with solution droplets of superior monodispersity is of the same order of magnitude as for the particles (see Fig. 3 and 4). However, there are also contributions due to different droplet trajectories in the ICP and by the mass distribution of the particles (the production company claimed a CV on the order of ~4.7%). Therefore, careful statistical evaluations of the average diameters of the particles and their size distributions have to be made in future studies applying, *e.g.*, high-resolution SEM in order to differentiate between the different sources of uncertainty.

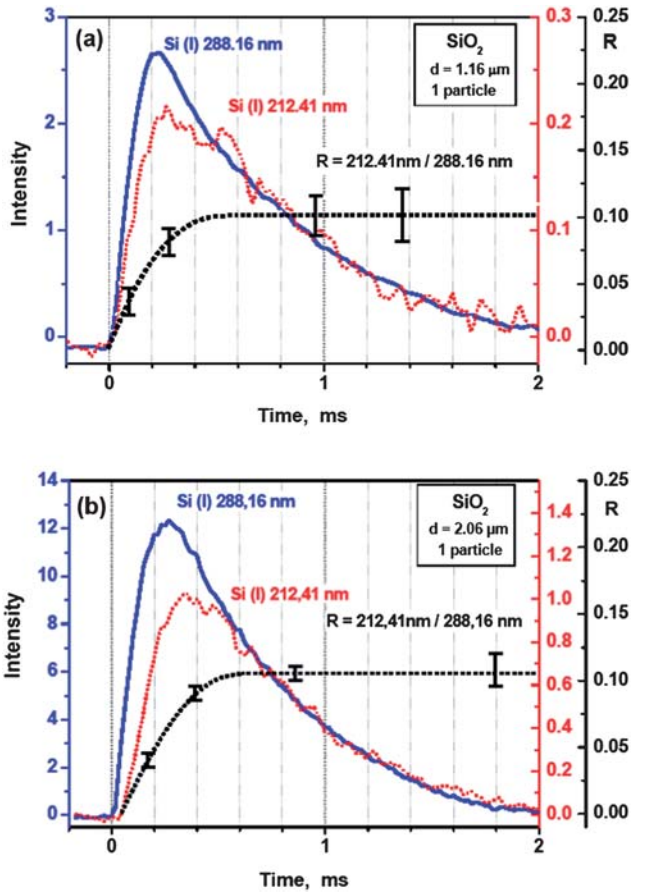

Fig. 5 The intensities of the 288.16 nm (left ordinate) and 212.41 nm (right ordinate) Si lines stemming from a low and a highly excited state, respectively, measured for droplets including (a) one 1.16 μm or (b) one 2.06 μm SiO_2 particle (time constant: 5.3 μs). The line intensity ratio R (dashed curve) is indicating the status of particle atomization. R becomes constant when the atomization is completed.

Complete atomization of particles in the ICP

The question, how large a SiO_2 particle can be to be completely atomized in the ICP at the relatively low Ar gas flow of 0.21 L min^{-1}, can be answered if the intensities of Si lines with different excitation energies are simultaneously measured. The criterion for complete atomization, first formulated in this journal[21] and demonstrated in Ref. 17, requires that "*the intensity ratios of ion and neutral lines, having different excitation energies and measured by end-on OES, reach time-independent, constant values*". Complete atomization is demonstrated in Fig. 5 where simultaneously measured intensities of the Si 288.16 nm (excitation energy: 40992 cm^{-1}) and 212.41 nm (excitation energy: 53362 cm^{-1}) lines and their ratio R are given for 1.16 μm and 2.06 μm SiO_2 particles. The intensity ratios R are reaching constant values (~0.1) in both cases indicating complete atomization. However, the increase of the ratio and the time when atomization is completed are slightly different for the two differently sized particles. The slower increase and the later time of complete atomization is both due to the larger mass of the 2.06 μm particle whose evaporation process cools the ICP locally more efficiently than smaller particles.[17] While the atomization of 0.83 μm particles (not shown in Fig. 5), was completed after ~0.4 ms, it took ~0.5, and ~0.6 ms for 1.16 μm and 2.06 μm particles, respectively. Note that the different times for complete atomization correspond to different positions in the ICP. It can be additionally seen in Fig. 5 that the positions of the peak intensities depend on the particle mass. This is even more obvious in Fig. 6 where the averaged intensities of the Si 288.16 nm line obtained with one, two and three particles of different size (0.83, 1.16, and 1.55 μm) in individual droplets are plotted in dependence on time. The temporal shift of the peak intensity with increasing particle mass can clearly be seen. The peak shift means that the vapor clouds producing the maxima have different positions in the ICP. However, different positions of the vapor cloud should lead to a measurable effect on the relative peak intensity in dependence on particle mass since the fixed optical imaging collects less emission from positions downstream the plasma. Therefore, the peak intensities recorded with large SiO_2 masses should be smaller than expected. Such deviation can be seen in Fig. 7 where the peak intensities measured with one, two and three particles of different diameter in single droplets are plotted against Si mass. While all data points lie on a straight line within the experimental errors, the peak values measured with one and two 2.06 μm SiO_2 particles are below that straight line, although 2.06 μm particles are completely atomized in the ICP at the experimental conditions used (see Fig. 5). The fact that the

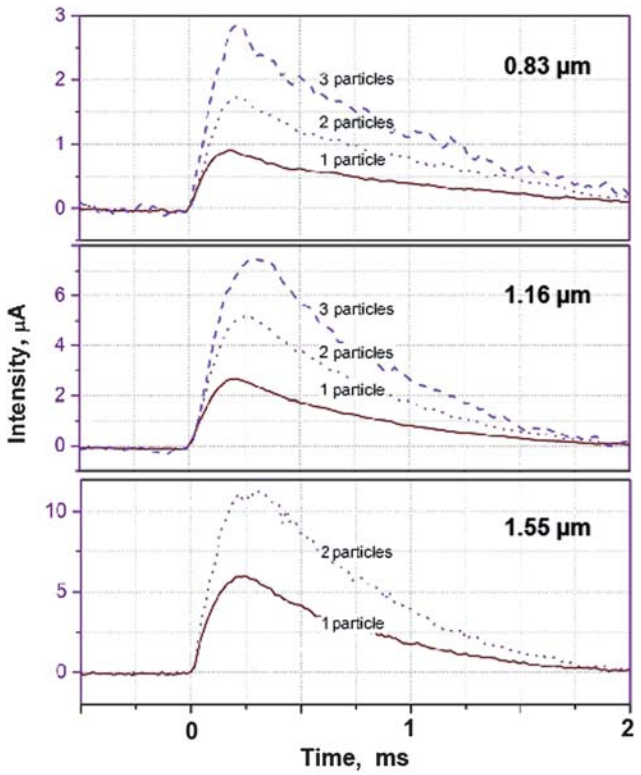

Fig. 6 The intensity of the Si 288.16 nm line measured with monodisperse droplets including SiO_2 particles (diameters: 0.83, 1.16, and 1.55 µm). For 0.83 and 1.16 µm particles the intensities of droplets with one, two and three particles in one droplet are given, while only the signals of droplets with one and two particles could be evaluated for the other particle sizes. Time constant: 5.3 µs.

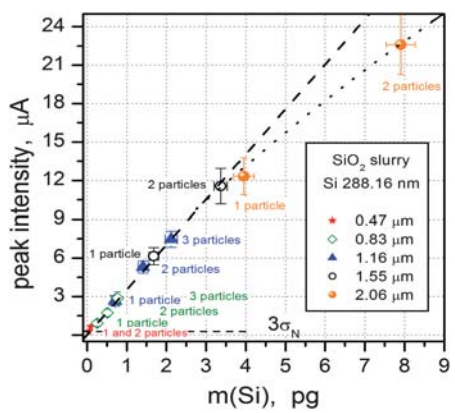

Fig. 7 Mass calibration obtained with suspensions including different SiO_2 particles (0.47, 0.83, 1.16, 1.55, and 2.06 µm). Peak signals obtained with droplets including 2 and 3 particles of each analyzed size are also plotted.

intensity ratio R of the 212.41nm/288.16 nm line becomes independent of time and agrees with the ratio measured with smaller particles (see Fig. 5) indicates that self-absorption cannot be the reason for the deviation of the 2.06 µm data points from the straight line in Fig. 7. Taking into account the intensities in Fig. 7, the spatial shift does not have a measurable effect on the peak intensity for Si masses below 3 pg which corresponds to the Si mass in two 1.55 µm SiO_2 particles.

It is very important to note that the spatial positions where the atomization of the analyte starts and is completed are approximately the same for droplets of analyte solutions, droplets of particle suspensions, and droplets of analyte solution including NPs. Furthermore, the droplet diameters should be about the same since the mass of the liquid in a droplet determines the desolvation time and, thus, the position in the ICP. If these conditions are fulfilled, the proposed characterization method for NPs in liquids can be applied. On the other hand, the atomization of dry airborne particles or particles from desolvated droplets made from analyte solutions starts earlier in the ICP than for analytes which are introduced as droplets to the ICP-OES. As a consequence, systematic errors in particle characterization are expected if line emission from dry, airborne particles is calibrated by monodisperse droplets of known size and analyte concentration.

The detection limit for SiO_2 particles using the Si 288.16 nm line was equivalent to the mass of a 470 nm particle (see Fig. 7). The Si mass in a 470 nm SiO_2 particle is ~50 fg.

Characterization of 250 nm Au particles

The largest Au particles which are commercially available with acceptable monodispersity have diameters of 250 nm. Taking into account the density of gold (19.3 g cm^{-3}), the mass of a single 250 nm particle amounts to 158 fg. Using the 267.59 nm Au line for detection, the peak intensities generated by 250 nm Au particles were about a factor of 2 higher than the detection limit ($3\sigma_N$-criterion). This means that our ICP-OES arrangement is able to measure Au masses as low as ~80 fg or to detect Au nanospheres with diameters larger than 200 nm.

The Au particle suspension was diluted by a factor of about 33 using deionized water and treated in the ultrasonic bath before droplet generation as it was done before with the SiO_2 particle suspensions. Also in the same way as in the SiO_2 experiment, small trace concentrations of Ca in the commercial suspension allowed using the Ca II line at 393.36 nm as an internal marker. Fig. 8 shows a histogram of 452 Au peak intensities generated by the atomized NPs. The distributions due to one and two particles in single droplets can be distinguished although the statistics is not as good as in the SiO_2 particle measurement displayed in Fig. 3 where more peaks were recorded. Nevertheless, one can see that the averaged peak intensities of the signals from one and two particles scale as 1 : 2 as expected.

Subsequently, the particle signals were calibrated with monodisperse droplets of gold standard solution having diameters of 47 µm. The Au concentration and mass in the droplets were relatively high (100 µg mL^{-1}, mass: 5.4 pg) and the signals of the solution droplets were, therefore, much larger than the particle signals. This can be seen in Fig. 9 where the averaged intensities of solution droplets and of droplets with one and two Au particles are given. The slower increase of the intensities than in the SiO_2 experiment is due to a larger time constant (0.53 ms) applied. The decrease of the particle signals below zero is due to the reduction of the ICP background intensity by the atomization and dissociation process of the water droplet as discussed in our recent paper.[17] Despite the relatively large differences of solution and particle signals, a detailed evaluation of the measured peak intensities and area intensities and a comparison

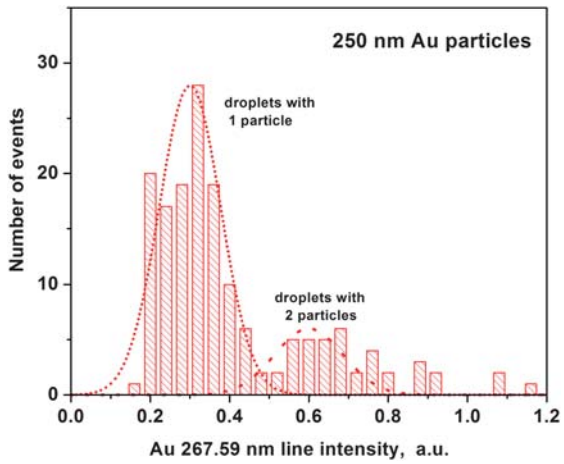

Fig. 8 Peak intensity distribution of the Au 267.59 nm line measured with a suspension of spherical 250 nm gold particles introduced into the ICP in 52 μm droplets. The commercially available suspension was diluted so that mostly one particle could be found in particle containing droplets.

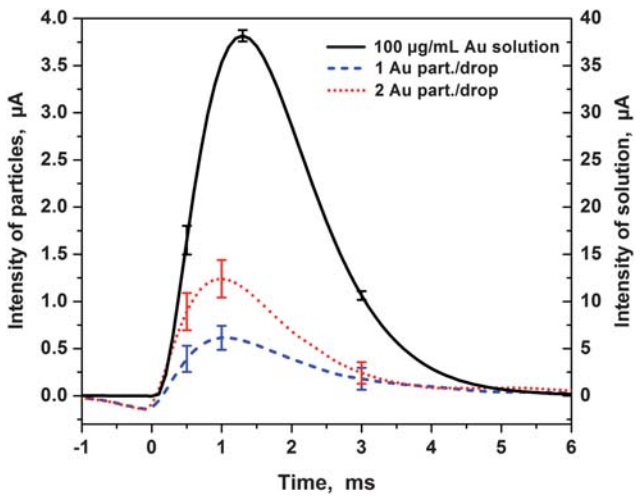

Fig. 9 Averaged intensities of the Au 267.59 nm line measured with one and two spherical 250 nm Au particles in monodisperse droplets from a suspension and with 47 μm droplets of a 100 μg mL^{-1} Au solution. The time constant was 0.53 ms.

with the expected Au mass ratios revealed that there was agreement between the particle and the solution signals within the mutual experimental errors.

In a further experiment, the diluted Au particle suspension was mixed with a gold standard solution, so that droplets of the Au concentration gave intensity signals being of the same order of magnitude as the signals generated by droplets with Au particles. Fig. 10 presents typical result as measured with the Au particles in a 3 μg mL^{-1} Au solution. The first intensity distribution corresponds to 49 μm droplets of the gold solution while the second represents the droplets of the solution with one Au particle included. The distribution of solution droplets with two particles can also be seen. However, their statistics are not good enough for evaluation. Taking into account the diameter and the Au concentration in the droplets, the Au mass in a single droplet

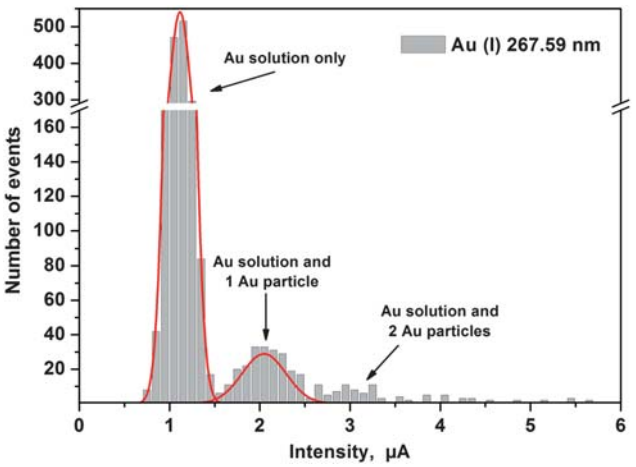

Fig. 10 Histogram of the peak intensities of the Au 267.59 nm line measured by ICP-OES with monodisperse 49 μm droplets of a 3 μg mL^{-1} Au solution without and with 250 nm Au particles.

without particles is 185 fg and 343 fg (185 fg + 158 fg) in droplets with one particle. The peak of the intensity distribution caused by droplets without particle was determined to be at 1.12 μA while it was at 2.05 μA for droplets of the solution including one particle. It means that excellent agreement between measured and expected peak intensity ratios was found. The measured peak ratio was 2.05 : 1.12 = 1.83, the ratio of Au masses in solution droplets with one particle to the Au mass in a solution droplets without a particle was 343 : 185 = 1.85.

It has to be stressed that our evaluations rely again on the correctness of the average diameter of the Au nanoparticles and its standard deviation of ±8% quoted by the commercial supplier. As already mentioned in the above section on SiO_2 particle measurements, the peak of a symmetrical particle size distribution with a coefficient of variation of a few percent is at a slightly smaller diameter as the peak of the corresponding mass distribution with is measured by ICP-OES. In the case of the droplets the coefficient of size variation is very small and the peaks of the size and mass distributions are practically the same. This has to be kept in mind in the evaluation of the measured line intensities. Therefore, also in the case of the 250 nm Au particles a careful statistical evaluation of the average particle diameter and the particle size distribution by high-resolution SEM is necessary to discriminate between the different sources of error (signal noise, different flight trajectories, and coefficient of size variation).

Simultaneous characterization of particles with different mass

A useful method for nano- and microparticle characterization in particle suspensions should be able to discriminate between particles of different mass. The precondition of such a measurement is that the probability to have more than one particle per droplet has to be so low that such events can be neglected. The Poisson statistics (see above) tells us how strong a particle suspension should be diluted. In order to demonstrate the possibility to measure particles of different masses, a SiO_2 particle suspension with monodisperse particles of three different sizes was prepared and further diluted than for the measurements

reported above. The diameter of the droplets used in this investigation was 52 μm. Histograms of the measured distributions of the peak intensities (lower graph) and the intensity areas (upper graph) for 0.83, 1.16 and 1.55 μm SiO_2 particles are shown in Fig. 11. The histograms are based on 45080 injected droplets at 20 Hz (total measurement time: 37 min and 34 s) with 247, 366, and 279 signals representing the 0.83 μm, 1.16 μm, and 1.55 μm particles, respectively. Obviously, there are only very few signals which are due to more than one particle in one droplet. The number of signals in the distributions at ~9 μA ms (area plot) or ~9.5 μA (peak intensity plot) representing droplets with two 1.55 μm particles is about two orders of magnitude lower than the number representing droplets with only one 1.55 μm particle. Following Poisson statistics, a further n-times dilution would reduce the probability of finding two particles instead of one particle in the droplets by n^{-1}. However, the measurement time would be n-times longer if distributions for single particles with comparable statistics as shown in Fig. 11 are wanted. The droplet injection frequency can certainly be further increased. However, one has to be aware that there are local plasma perturbations by the evaporation and atomization process of the liquid (here: water) which was studied recently.[17] A possibility to shorten the analysis time by applying higher droplet injection frequencies without perturbation by the liquid can only be accomplished by reducing the mass of the droplet, *i.e.*, by generation of droplets with diameter <40 μm (see Ref. 17). In that case, the droplet injection frequency is limited by the length of the analyte signals which is about 2 ms at the present experimental conditions. It means that injection frequencies larger than 500 Hz should not be applied even when the droplets are smaller than 40 μm. However, in view of NP analysis by ICP-MS, ion signals much shorter than 1 ms are expected since the duration is given by the size of the analyte clouds and their transport velocity. This means that droplet injection frequencies of the order of 1 kHz or higher can be applicable which helps to shorten the analysis time significantly.

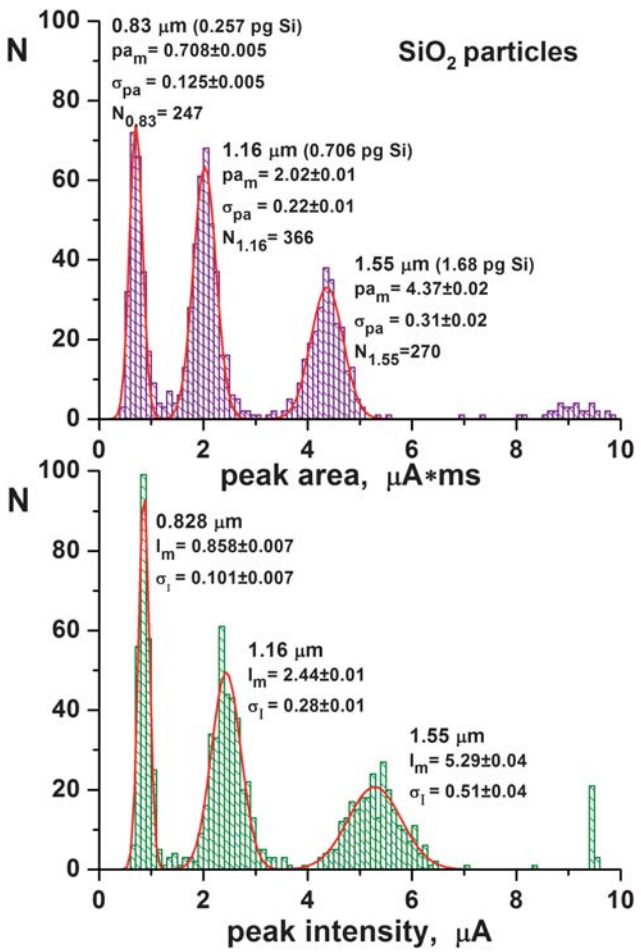

Fig. 11 ICP-OES measurements of 52 μm droplets generated from a diluted suspension including monodisperse 0.83 μm, 1.16 μm and 1.55 μm SiO_2 particles. The Si line used for detection was 288.16 nm. The total number of droplets injected was 45080.

It has to be mentioned that the ratios of the averaged peak intensities or peak areas (given in Fig. 11 together with the experimental uncertainties as I_m and pa_m, respectively) are in very good agreement with the nominal mass ratios of the SiO_2 particles. The Si masses in the 0.83 μm, 1.16 μm, and 1.55 μm particles are 0.26 pg, 0.71 pg, and 1.68 pg, respectively. The corresponding mass ratios 0.26/0.71 and 0.26/1.7 are 0.37 and 0.15. The averaged values of the measured peak intensities and peak areas were 0.86 μA and 0.71 μA ms (0.83 μm), 2.4 μA and 2.0 μA ms (1.16 μm), and 5.3 μA and 4.4 μA ms (1.55 μm). Therefore, the experimental ratios of the averaged peak intensities and peak areas obtained for the 0.83 μm/1.16 μm particles are both 0.36, while 0.16 was found for the 0.83 μm/1.55 μm mass ratio evaluating both the peak intensities as well as the peak areas.

The width of the intensity distributions is a measure for the ability to discriminate particle masses applying the present ICP-OES arrangement. Taking into account the widths of the intensity distributions, it should be possible to separate signals of SiO_2 particles having masses which differ by 10 to 20%. We believe that mass discrimination can even be better if the effect of different droplet/particle trajectories can be reduced as discussed above.

In view of the application of ICP-MS for chemical characterization of NPs the effect of slightly different particle trajectories should not be as severe as in end-on ICP-OES since the vapor clouds of the analyzed particles are already expanded by diffusion when they arrive at the sampling orifice of the mass spectrometer.

Conclusion

The results presented here demonstrate that calibration of atomic or ionic line emission from atomized nano- and microparticles in droplets by the line emission from monodisperse solution droplets of known size and element composition seems to be possible. It is a new technique for NP characterization in liquids. However, it could also be used for characterization of airborne NPs if these particles are collected and implemented to a liquid before analysis.

Measurements with monodisperse 250 nm Au and SiO_2 particles of different sizes revealed $3\sigma_N$ detection limits of ~80 fg (Au) and ~50 fg (Si) using strong emission lines of the elements. These detection limits correspond to ~200 nm and ~470 nm spherical gold and SiO_2 particles, respectively. It was shown that

particles having 10–20% different masses can be discriminated by ICP-OES. The discrimination is limited by the uncertainty of the intensity measurement which is mainly due to different trajectories of the droplets/particles in the plasma if the intensities are much larger than the noise of the background.

Finally, the authors do not see any reason why the new calibration method for NPs in suspensions is not transferable to ICP-MS. Since ICP-MS delivers typically three orders of magnitude better detection limits for most elements accessible by ICP spectrometry, chemical characterization of particles with masses in the attogram range should be possible.

Acknowledgements

Project funding by the Deutsche Forschungsgemeinschaft (DFG) is gratefully acknowledged. The authors also thank the Ministry of Innovation, Science, Research and Technology of the state Northrhine-Westphalia and the Ministry of Education and Research of the Federal Republic of Germany for general support, and Dr Alex von Bohlen and Mrs. Maria Becker for SEM measurements of the particle size distributions.

References

1 D. Astruc, *Nanoparticles and Catalysis*, Wiley-VCH Verlag, Weinheim, 2008.
2 J. Fan and Y. Gao, *J. Exp. Nanosci.*, 2006, **1**, 457–475.
3 G. A. Somorjai and J. Y. Park, *Top. Catal.*, 2008, **49**, 126–135.
4 K. Ramaratnam, S. K. Iyer, M. K. Kinnan, G. Chumanov, P. J. Brown and I. Luzinov, *J. Engineered Fibers and Fabrics*, 2008, **3**, 1–14.
5 M. R. Gwinn and V. Vallyathan, *Environ. Health Perspect.*, 2006, **114**, 1818–1825.
6 R. E. Hester, R. M. Harrison, *Nanotechnology -Consequences for Human Health and the Environment*, R.S.C., Cambridge, UK, 2008.
7 W. H. De Jong, W. I. Hagens, P. Krystek, M. C. Burger, A. J. A. M. Sips and R. E. Geertsma, *Biomaterials*, 2008, **29**, 1912–1919.
8 M. Hosokawa, K. Nogi, M. Naito, T. Yokoyama, *Nanoparticle Technology Handbook*, Elsevier, 2008.
9 D. J. Burleson, M. D. Driessen and R. Lee Penn, *J. Environ. Sci. Health, Part A: Toxic/Hazard. Subst. Environ. Eng.*, 2005, **39**, 2707–2753.
10 M. Weiss, P. J. T. Verheijen, J. C. M. Marijnissen and B. Scarlett, *J. Aerosol Sci.*, 1997, **28**, 159–171.
11 D. A. Cremers and L. Radziemski, *Appl. Spectrosc.*, 1985, **39**, 57–63.
12 D. W. Hahn, J. E. Carranza, G. R. Arsenault, H. A. Johnsen and K. R. Hencken, *Rev. Sci. Instrum.*, 2001, **72**, 3706–3713.
13 V. Hohreiter and D. W. Hahn, *Anal. Chem.*, 2006, **78**, 1509–1514.
14 H. Kawaguchi, N. Fukasawa and A. Mizuike, *Spectrochim. Acta, Part B*, 1986, **41**, 1277–1286.
15 K. Knight, S. Chenery, S. W. Zochowski, M. Thompson and C. D. Flint, *J. Anal. At. Spectrom.*, 1996, **11**, 53–56.
16 J. W. Olesik, *Appl. Spectrosc.*, 1997, **51**, 158A–175A.
17 S. Groh, C. C. Garcia, A. Murtazin, V. Horvatic and K. Niemax, *Spectrochim. Acta, Part B*, 2009, **64**, 247–254.
18 M. Miclea, C. C. Garcia, I. Exius, H. Lindner and K. Niemax, *Spectrochim. Acta, Part B*, 2006, **61**, 361–367.
19 J. W. Olesik and S. E. Hobbs, *Anal. Chem.*, 1994, **66**, 3371–3378.
20 S. Groh, P. Diwakar, C. C. Garcia, A. Murtazin, K. Niemax, D. Hahn, submitted for publication.
21 C. C. Garcia, H. Lindner and K. Niemax, *J. Anal. At. Spectrom.*, 2009, **24**, 14–25.